Proceedings of the ASME 2016 Dynamic Systems and Control Conference
DSCC 2016
October 12-14, 2016, Minneapolis, Minnesota, USA

DSCC2016-9877

STATE ESTIMATION FOR AN ELECTROCHEMICAL MODEL OF MULTIPLE-MATERIAL LITHIUM-ION BATTERIES

Leobardo Camacho-Solorio
Miroslav Krstic
Mechanical and Aerospace Engineering
University of California, San Diego
La Jolla, California 92093
lcamacho@ucsd.edu,
krstic@ucsd.edu

Reinhardt Klein
Anahita Mirtabatabaei
Robert Bosch LLC
Palo Alto, California 94304
reinhardt.klein@us.bosch.com,
Anahita.MirTabatabaei@us.bosch.com

Scott J. Moura
Civil and Environmental Engineering
University of California, Berkeley
Berkeley, California 94720
smoura@berkeley.edu

ABSTRACT

This paper presents state estimation for a system of diffusion equations coupled in the boundary appearing in reduced electrochemical models of lithium-ion batteries with multiple active materials in single electrodes. The observer is synthesized from a single particle model and is based on the backstepping method for partial differential equations. The observer is suitable for state of charge estimation in battery management systems and is an extension of existing backstepping observers which were derived only for cells with electrodes of single active materials. Observer gains still can be computed analytically in terms of Bessel and modified Bessel functions. This extension is motivated by the trend in cell manufacturing to use multiple active materials to combine power and energy characteristics or reduce degradation.

1 Introduction

Accurate battery estimation algorithms are of great importance due to their application in consumer electronics, electrified transportation and energy storage systems for renewable sources. Electrochemical model-based estimation provides visibility into operating regimes that induce degradation enabling a larger domain of operation to increase performance with respect to energy capacity, power capacity and fast charge rates [1]. Electrochemical model-based estimation is challenging for several reasons. First, measurements of lithium concentrations outside specialized laboratory environments is impractical [2]. Second, the concentration dynamics are governed by partial differential algebraic equations (PDAE) [3]. Finally, the only measurable quantities (voltage and current) are related to dynamic states through a nonlinear function. Manufacturers are using multiple active materials in the positive electrode of lithium-ion cells to combine power and energy characteristics or reduce degradation. For example, $Li_yMn_2O_4$ is a promising positive-electrode material because of its high potential, high rate capability, abundance and low cost [4, 5]. However, $Li_yMn_2O_4$ has problems with the dissolution of Mn and its migration to the negative electrode where it increases the rate of side reactions and reduces cell life [4, 5]. Adding a layered oxide material such as $Li_yNi_{0.80}Co_{0.15}Al_{0.05}O_2$ in the positive electrode can reduce the rate of dissolution and cells with a mixture of these two positive-electrode materials are now being produced commercially [4].

WHAT ?

1.1 Relevant Literature

Over the past decade, the engineering literature on battery estimation has grown considerably rich with various algorithms, models, and applications. One may categorize this literature by the battery models each algorithm employs.

The first category utilizes equivalent circuit models (ECMs). These models use circuit elements to mimic the phenomenological behavior of batteries [6]. The seminal paper by Plett [7] was one of the first to apply extended Kalman filtering (EKF) to ECMs for simultaneous state and parameter estimation. Over the past

decade, a variety of ECM-based algorithms have been developed, including linear parameter varying observers [8], sliding mode observers [9], polynomial chaos [10], unscented Kalman filters [11], and particle filters [12].

The second category of literature considers electrochemical models, which account for the diffusion, intercalation, and electrochemical kinetics. Although these models can accurately predict internal state variables, their mathematical structure renders observer design challenging. Consequently, most approaches develop estimators for reduced-order models. Among the various reduced models the single particle model (SPM) has been widely used for estimation [13–16] including extensions to account for electrolyte dynamics [17–20] and for electrodes with multiple active materials [21].

1.2 Main Contributions

The main contributions of this paper are the following:

1. A derivation of a single particle model for lithium-ion batteries with multiple active materials in single electrodes.
2. An observer based on the backstepping method for partial differential equations [22] suitable for state of charge estimation. This observer is an extension of backstepping observers for electrodes of a single active material [15, 20, 23].

1.3 Outline

The remainder of the paper is organized as follows. First, section 2 derives a single particle model for lithium-ion batteries with multiple active materials in single electrodes. Then, section 3 presents the derivation of an observer suitable for state of charge estimation. After that, simulation results are provided in section 4. Finally, conclusions are listed in section 5.

2 Model Derivation

First, an extension of the Doyle-Fuller-Newman (DFN) model [1, 3] for cells with multiple active materials is described briefly. This extension follows results in [4] and describes the dynamic behavior of a cell with n^+ active materials in the positive electrode and n^- active materials in the negative electrode. Modifications to the original DFN model are the following. Diffusion of lithium in solid phase is described independently for each material

$$\frac{\partial c_{\mathrm{s},i}}{\partial t}(x,r,t) = \frac{1}{r^2}\frac{\partial}{\partial r}\left[D_{\mathrm{s},i} r^2 \frac{\partial c_{\mathrm{s},i}}{\partial r}(x,r,t)\right], \tag{1}$$

$$\frac{\partial c_{\mathrm{s},i}}{\partial r}(x,0,t) = 0, \tag{2}$$

$$D_{\mathrm{s},i}\frac{\partial c_{\mathrm{s},i}}{\partial r}(x,R_{\mathrm{p},i},t) = -j_{\mathrm{n},i}(x,t), \tag{3}$$

with $i \in \{1^-, 2^-, ..., n^-, 1^+, ..., n^+\}$. A unique molar ion flux $j_{\mathrm{n},i}(x,t)$ should be computed for each material

$$j_{\mathrm{n},i}(x,t) = \frac{i_{0,i}(x,t)}{F}\left[e^{\frac{\alpha_{\mathrm{a}}F}{RT}\eta_i(x,t)} - e^{-\frac{\alpha_{\mathrm{c}}F}{RT}\eta_i(x,t)}\right], \tag{4}$$

where $c_{\mathrm{ss},i}(x,t) = c_{\mathrm{s},i}(x,R_{\mathrm{p},i},t)$ and

$$i_{0,i}(x,t) = k_i\left[c_{\mathrm{ss},i}(x,t)\right]^{\alpha_{\mathrm{c}}}\left[c_{\mathrm{e}}(x,t)\left(c_{\mathrm{s}\max,i} - c_{\mathrm{ss},i}(x,t)\right)\right]^{\alpha_{\mathrm{a}}}, \tag{5}$$

$$\begin{aligned}\eta_i(x,t) = {} & \phi_{\mathrm{s}}(x,t) - \phi_{\mathrm{e}}(x,t) - U_i(c_{\mathrm{ss},i}(x,t)) \\ & - R_{\mathrm{f},i}F j_{\mathrm{n},i}(x,t).\end{aligned} \tag{6}$$

Charge conservation in electrodes becomes

$$\frac{\partial i_{\mathrm{e}}}{\partial x}(x,t) = \sum_k a_{\mathrm{s},k} F j_{\mathrm{n},k}(x,t), \tag{7}$$

where the sum is over all materials in each electrode, $a_{\mathrm{s},i} = 3\varepsilon_{\mathrm{s},i}/R_{\mathrm{p},i}$ is the specific interfacial area and $\varepsilon_{\mathrm{s},i}$ is the volume fraction of each active material in the corresponding electrode. Equations for lithium concentration in the electrolyte $c_{\mathrm{e}}(x,t)$, solid electric potential $\phi_{\mathrm{s}}(x,t)$ and electrolyte electric potential $\phi_{\mathrm{e}}(x,t)$ remain unchanged

$$\frac{\partial c_{\mathrm{e}}}{\partial t}(x,t) = \frac{\partial}{\partial x}\left[D_{\mathrm{e}}\frac{\partial c_{\mathrm{e}}}{\partial x}(x,t) + \frac{1-t_{\mathrm{c}}^0}{\varepsilon_{\mathrm{e}}F} i_{\mathrm{e}}(x,t)\right], \tag{8}$$

$$\frac{\partial \phi_{\mathrm{s}}}{\partial x}(x,t) = \frac{I(t) - i_{\mathrm{e}}(x,t)}{\sigma}, \tag{9}$$

$$\begin{aligned}\frac{\partial \phi_{\mathrm{e}}}{\partial x}(x,t) = {} & \frac{i_{\mathrm{e}}(x,t)}{\kappa} + \frac{2RT}{F}(1-t_{\mathrm{c}}^0) \\ & \times\left(1 + \frac{d\ln f_{\mathrm{c/a}}}{d\ln c_{\mathrm{e}}}(x,t)\right)\frac{\partial \ln c_{\mathrm{e}}}{\partial x}(x,t).\end{aligned} \tag{10}$$

Notice that solid and electrolyte electric potential have the same value for all materials in the same electrode. Boundary conditions for the electrolyte-phase diffusion PDE (8) are given by

$$\frac{\partial c_{\mathrm{e}}}{\partial x}(0^-,t) = \frac{\partial c_{\mathrm{e}}}{\partial x}(0^+,t) = 0, \tag{11}$$

$$\frac{\partial c_{\mathrm{e}}}{\partial x}(L^-,t) = \frac{\varepsilon_{\mathrm{e,sep}} D_{\mathrm{e}}(0^{\mathrm{sep}})}{\varepsilon_{\mathrm{e},-} D_{\mathrm{e}}(L^-)}\frac{\partial c_{\mathrm{e}}}{\partial x}(0^{\mathrm{sep}},t), \tag{12}$$

$$\frac{\partial c_{\mathrm{e}}}{\partial x}(L^{\mathrm{sep}},t) = \frac{\varepsilon_{\mathrm{e},+} D_{\mathrm{e}}(L^+)}{\varepsilon_{\mathrm{e,sep}} D_{\mathrm{e}}(L^{\mathrm{sep}})}\frac{\partial c_{\mathrm{e}}}{\partial x}(L^+,t), \tag{13}$$

$$c_{\mathrm{e}}(L^-,t) = c_{\mathrm{e}}(0^{\mathrm{sep}},t), \tag{14}$$

$$c_{\mathrm{e}}(L^{\mathrm{sep}},t) = c_{\mathrm{e}}(L^+,t). \tag{15}$$

Boundary conditions for the solid-phase potential ODE (9) are given by

$$\frac{\partial \phi_s}{\partial x}(L^-,t) = \frac{\partial \phi_s}{\partial x}(L^+,t) = 0. \tag{16}$$

Boundary conditions for the electrolyte-phase potential ODE (10) are given by

$$\phi_e(0^-,t) = 0, \tag{17}$$
$$\phi_e(L^-,t) = \phi_e(0^{sep},t), \tag{18}$$
$$\phi_e(L^{sep},t) = \phi_e(L^+,t). \tag{19}$$

Boundary conditions for the ionic current ODE (7) are given by

$$i_e(0^-,t) = i_e(0^+,t) = 0, \tag{20}$$

and $i_e(x,t) = I(t)$ for $x \in [0^{sep}, L^{sep}]$. The input to the model is the applied current density $I(t)$ (with positive values used for discharging) and the output is the voltage measured across the current collectors,

$$V(t) = \phi_s(0^+,t) - \phi_s(0^-,t). \tag{21}$$

The main assumptions used to derive the SPM model for electrodes with multiple materials are the following

[A1]: Lithium concentration in both electrodes is constant in space, uniformly in time. Mathematically, $c_{s,i}(x,t)$ and $j_{n,i}(x,t)$ are constant in the x direction.
[A2]: The term $i_{0,i}(x,t)$ can be approximated by its averaged value $i_{0,i}(t)$, which is independent of x.
[A3]: Lithium concentration is constant in space and time, i.e. $c_e(x,t) = c_{e,0}$.

This ultimately renders a model consisting of: (i) a set of $n^- + n^+$ spherical diffusion PDEs modeling concentration in each active material, (ii) a set of nonlinear algebraic equations and (iii) a nonlinear output function mapping boundary values of solid concentration and molar fluxes to terminal voltage. The resulting SPM equations are the following. Using assumption **[A1]** solid diffusion equations are

$$\frac{\partial c_{s,i}}{\partial t}(r,t) = \frac{1}{r^2}\frac{\partial}{\partial r}\left[D_{s,i} r^2 \frac{\partial c_{s,i}}{\partial r}(r,t)\right], \tag{22}$$
$$\frac{\partial c_{s,i}}{\partial r}(0,t) = 0, \tag{23}$$
$$D_{s,i}\frac{\partial c_{s,i}}{\partial r}(R_{p,i},t) = -j_{n,i}(t), \tag{24}$$

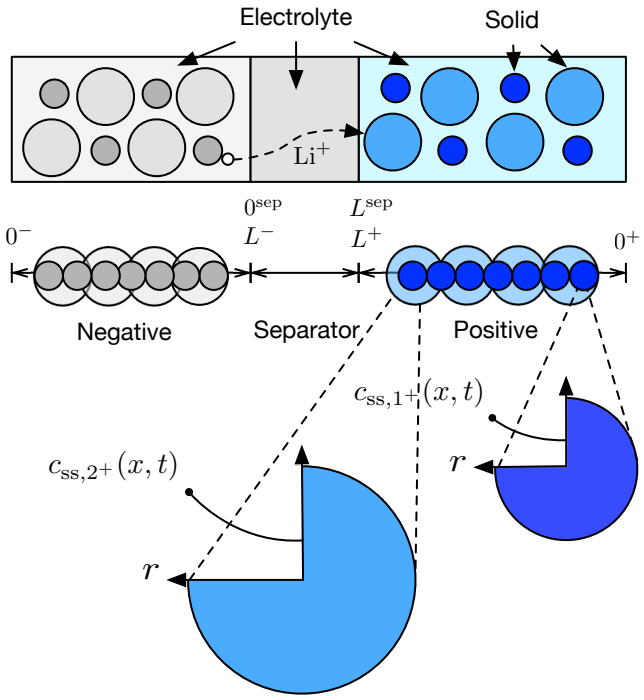

FIGURE 1. DFN SCHEMATIC. Schematic of Doyle-Fuller-Newman (DFN) model for electrodes with multiple active materials. This is a two-dimensional model with two phases: solid and electrolyte. States in the solid evolve in x and r dimensions while states in electrolyte evolve only in the x dimension. The cell is divided in three subdomains: negative electrode, separator and positive electrode.

where the solid-phase concentration no longer depends on x. Using assumption **[A1]** and boundary conditions (20) charge conservation becomes

$$I(t) = \sum_{k=1^-}^{n^-} a_{s,k} F L^- j_{n,k}(t), \tag{25}$$
$$I(t) = -\sum_{k=1^+}^{n^+} a_{s,k} F L^+ j_{n,k}(t). \tag{26}$$

From assumptions **[A1]**, **[A2]** and **[A3]** Butler-Volmer equation in (4) becomes

$$j_{n,i}(t) = \frac{i_{0,i}(t)}{F}\left[e^{\frac{\alpha_a F}{RT}\eta_i(t)} - e^{-\frac{\alpha_c F}{RT}\eta_i(t)}\right], \tag{27}$$
$$i_{0,i}(t) = k_i\left[c_{ss,i}(t)\right]^{\alpha_c}\left[c_{e,0}\left(c_{s,\max,i} - c_{ss,i}(t)\right)\right]^{\alpha_a}, \tag{28}$$

with $c_{ss,i}(t) = c_{s,i}(R_{p,i},t)$. Solid electric potential is constant over each electrode and equal for all materials within the same elec-

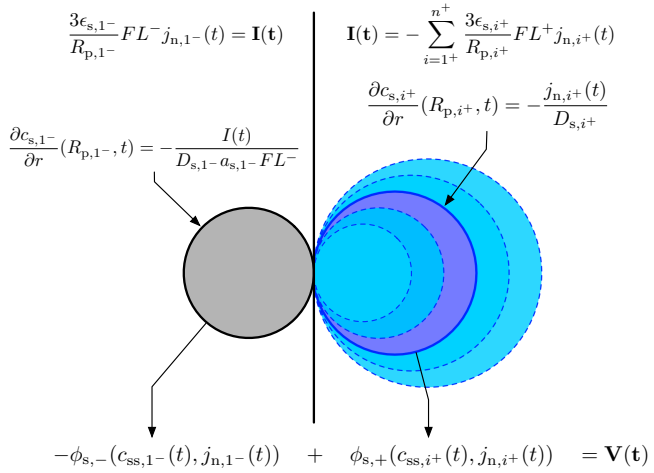

FIGURE 2. SPM SCHEMATIC. Schematic of single particle model for one material in the negative electrode and n^+ materials in the positive electrode. This a common configuration of commercial lithium-ion batteries where graphite is used for the negative electrode and a mixture of multiple active materials is used in the positive electrode.

trode, therefore any index i^- or i^+ can be used to compute $\phi_{s,-}(t)$ or $\phi_{s,+}(t)$ respectively, i.e.

$$\phi_{s,-}(t) = \eta_{i^-},(t) + U_{i^-}(c_{ss,i^-}(t)) + R_{f,i^-} F j_{n,i^-}(t), \quad (29)$$
$$\phi_{s,+}(t) = \eta_{i^+},(t) + U_{i^+}(c_{ss,i^+}(t)) + R_{f,i^+} F j_{n,i^+}(t). \quad (30)$$

Finally, output voltage is computed as

$$V(t) = \phi_{s,+}(t) - \phi_{s,-}(t). \quad (31)$$

Proposition 1. *Lithium in the solid phase is conserved [24]. Mathematically,* $\frac{d}{dt} n_{Li,s}(t) = 0$ *where*

$$n_{Li,s}(t) = \sum_i \frac{\varepsilon_{s,i} L_i}{\frac{4}{3}\pi R_{s,i}^3} \int_0^{R_{p,i}} 4\pi r^2 c_{s,i}(r,t) dr \quad (32)$$

where the sum is computed over all active materials in both electrodes.

The proof is straight-forward and omitted for brevity. In the following observer estimation gains are selected to conserve lithium in solid phase.

3 State Observer Design

In this section an observer is developed for a cell with one active material in the negative electrode and two active materials in the positive electrode, see Fig. 2. Extension to more active materials in the positive electrode is straightforward. The observer design process is summarized as follows:

1. Linearization of algebraic equations in the positive electrode
2. Normalization and state transformation of solid diffusion equations in the positive electrode
3. Derivation of backstepping PDE observer for the transformed solid diffusion system
4. Inverse state transformation and un-normalization
5. Derivation of an observer in the negative electrode to conserve lithium in solid

3.1 Linearization of Algebraic Equations

First, a linear approximation of the dynamic and algebraic states in the positive electrode is being considered

$$\phi_{s,+}(t) = U_{i^+}(c^{eq}_{s,i^+}) + \widetilde{\phi}_{s,+}(t), \quad (33)$$
$$c_{ss,1^+}(t) = c^{eq}_{s,1^+} + \widetilde{c}_{ss,1^+}(t), \quad (34)$$
$$c_{ss,2^+}(t) = c^{eq}_{s,2^+} + \widetilde{c}_{ss,2^+}(t), \quad (35)$$
$$j_{n,1^+}(t) = \widetilde{j}_{n,1^+}(t), \quad (36)$$
$$j_{n,2^+}(t) = \widetilde{j}_{n,2^+}(t), \quad (37)$$

around the equilibrium $(U_{i^+}(c^{eq}_{s,i^+}), c^{eq}_{s,1^+}, c^{eq}_{s,2^+}, 0, 0)$ to find a linear approximation of the algebraic equation in (26) and the pair of algebraic equations in (30) (one for each active material)

$$I(t) = -\frac{3\varepsilon_{s,1^+}}{R_{p,1^+}} FL\widetilde{j}_{n,1^+}(t) - \frac{3\varepsilon_{s,2^+}}{R_{p,2^+}} FL\widetilde{j}_{n,2^+}(t). \quad (38)$$

$$0 = -\widetilde{\phi}_{s,+}(t) + \frac{RT\widetilde{j}_{n,1^+}(t)}{(\alpha_a + \alpha_c) i_{0,1^+}(t)} + R_{f,1^+} F\widetilde{j}_{n,1^+}(t) + \frac{\partial U_{1^+}}{\partial c_{ss,1^+}}\left(c^{eq}_{s,1^+}\right)\widetilde{c}_{ss,1^+}(t), \quad (39)$$

$$0 = -\widetilde{\phi}_{s,+}(t) + \frac{RT\widetilde{j}_{n,2^+}(t)}{(\alpha_a + \alpha_c) i_{0,2^+}(t)} + R_{f,2^+} F\widetilde{j}_{n,2^+}(t) + \frac{\partial U_{2^+}}{\partial c_{ss,2^+}}\left(c^{eq}_{s,2^+}\right)\widetilde{c}_{ss,2^+}(t), \quad (40)$$

and then solve for $\widetilde{j}_{n,1^+}(t)$ and $\widetilde{j}_{n,2^+}(t)$ in terms of $\widetilde{c}_{ss,1^+}$, $\widetilde{c}_{ss,2^+}$ and $I(t)$

$$\widetilde{j}_{n,1^+}(t) = -\rho_{11}\widetilde{c}_{ss,1^+}(t) - \rho_{12}\widetilde{c}_{ss,2^+}(t) - \rho_1 I(t), \quad (41)$$
$$\widetilde{j}_{n,2^+}(t) = -\rho_{21}\widetilde{c}_{ss,1^+}(t) - \rho_{22}\widetilde{c}_{ss,2^+}(t) - \rho_2 I(t). \quad (42)$$

3.2 Normalization and State Transformation

Next normalization and state transformation is used to simplify the mathematical structure of the observer in the positive electrode. First scale the radial r and time t coordinates as follows

$$\bar{r} = \frac{r}{R_{\mathrm{p},i}}, \qquad \bar{t} = \frac{D_{\mathrm{s},i}}{(R_{\mathrm{p},i})^2} t. \tag{43}$$

Bars over the space and time coordinates will be dropped to simplify notation. Next state transformation is used to eliminate the first spatial derivative in the spherical diffusion Eqns. (22)

$$c_i(r,t) = r c_{\mathrm{s},i}(r,t). \tag{44}$$

This normalization and state transformation produces the following PDE

$$\frac{\partial}{\partial t}\begin{bmatrix} c_1 \\ c_2 \end{bmatrix}(r,t) = \frac{\partial^2}{\partial r^2}\begin{bmatrix} c_1 \\ c_2 \end{bmatrix}(r,t), \tag{45}$$

$$\begin{bmatrix} c_1 \\ c_2 \end{bmatrix}(0,t) = 0, \tag{46}$$

$$\frac{\partial}{\partial r}\begin{bmatrix} c_1 \\ c_2 \end{bmatrix}(1,t) - \begin{bmatrix} c_1 \\ c_2 \end{bmatrix}(1,t) = \begin{bmatrix} a_{11} & a_{12} \\ a_{21} & a_{22} \end{bmatrix}\begin{bmatrix} c_1 \\ c_2 \end{bmatrix}(1,t) + \begin{bmatrix} a_1 \\ a_2 \end{bmatrix} I(t). \tag{47}$$

where

$$a_{11} = \frac{R_{\mathrm{p},1^+}}{D_{\mathrm{s},1^+}}\rho_{11}, \quad a_{12} = \frac{R_{\mathrm{p},1^+}}{D_{\mathrm{s},1^+}}\rho_{12}, \tag{48}$$

$$a_{21} = \frac{R_{\mathrm{p},2^+}}{D_{\mathrm{s},2^+}}\rho_{21}, \quad a_{22} = \frac{R_{\mathrm{p},2^+}}{D_{\mathrm{s},2^+}}\rho_{22}, \tag{49}$$

$$a_1 = \frac{R_{\mathrm{p},1^+}}{D_{\mathrm{s},1^+}}\rho_1, \qquad a_2 = \frac{R_{\mathrm{p},2^+}}{D_{\mathrm{s},2^+}}\rho_2. \tag{50}$$

3.3 Backstepping Observer for Positive Electrode

The observer in the positive electrode is a copy of the plant (45)-(47) plus boundary state error injection

$$\frac{\partial}{\partial t}\begin{bmatrix} \widehat{c}_1 \\ \widehat{c}_2 \end{bmatrix}(r,t) = \frac{\partial^2}{\partial r^2}\begin{bmatrix} \widehat{c}_1 \\ \widehat{c}_2 \end{bmatrix}(r,t) + \begin{bmatrix} p_{11}(r) & p_{12}(r) \\ p_{21}(r) & p_{22}(r) \end{bmatrix}\begin{bmatrix} \widetilde{c}_1 \\ \widetilde{c}_2 \end{bmatrix}(1,t), \tag{51}$$

$$\begin{bmatrix} \widehat{c}_1 \\ \widehat{c}_2 \end{bmatrix}(0,t) = 0 \tag{52}$$

$$\frac{\partial}{\partial r}\begin{bmatrix} \widehat{c}_1 \\ \widehat{c}_2 \end{bmatrix}(1,t) - \begin{bmatrix} \widehat{c}_1 \\ \widehat{c}_2 \end{bmatrix}(1,t) = \begin{bmatrix} a_{11} & a_{12} \\ a_{21} & a_{22} \end{bmatrix}\begin{bmatrix} \widehat{c}_1 \\ \widehat{c}_2 \end{bmatrix}(1,t) + \begin{bmatrix} a_1 \\ a_2 \end{bmatrix} I(t) + \begin{bmatrix} q_{11} & q_{12} \\ q_{21} & q_{22} \end{bmatrix}\begin{bmatrix} \widetilde{c}_1 \\ \widetilde{c}_2 \end{bmatrix}(1,t) \tag{53}$$

where boundary estimation error is defined as $[\widetilde{c_1}, \widetilde{c_2}]^T(r,t) = [c_1, c_2]^T(r,t) - [\widehat{c_1}, \widehat{c_2}]^T(r,t)$ and values of surface concentration $[c_1, c_2]^T(r,t)$ are assumed to be known or are being estimated from measurements. The estimation error system is

$$\frac{\partial}{\partial t}\begin{bmatrix} \widetilde{c}_1 \\ \widetilde{c}_2 \end{bmatrix}(r,t) = \frac{\partial^2}{\partial r^2}\begin{bmatrix} \widetilde{c}_1 \\ \widetilde{c}_2 \end{bmatrix}(r,t) - \begin{bmatrix} p_{11}(r) & p_{12}(r) \\ p_{21}(r) & p_{22}(r) \end{bmatrix}\begin{bmatrix} \widetilde{c}_1 \\ \widetilde{c}_2 \end{bmatrix}(1,t), \tag{54}$$

$$\begin{bmatrix} \widetilde{c}_1 \\ \widetilde{c}_2 \end{bmatrix}(0,t) = 0 \tag{55}$$

$$\frac{\partial}{\partial r}\begin{bmatrix} \widetilde{c}_1 \\ \widetilde{c}_2 \end{bmatrix}(1,t) - \begin{bmatrix} \widetilde{c}_1 \\ \widetilde{c}_2 \end{bmatrix}(1,t) = \begin{bmatrix} a_{11} & a_{12} \\ a_{21} & a_{22} \end{bmatrix}\begin{bmatrix} \widetilde{c}_1 \\ \widetilde{c}_2 \end{bmatrix}(1,t) - \begin{bmatrix} q_{11} & q_{12} \\ q_{21} & q_{22} \end{bmatrix}\begin{bmatrix} \widetilde{c}_1 \\ \widetilde{c}_2 \end{bmatrix}(1,t) \tag{56}$$

The backstepping approach seeks to find the upper-triangular transformation

$$\begin{bmatrix} \widetilde{c}_1 \\ \widetilde{c}_2 \end{bmatrix} = \begin{bmatrix} w_1 \\ w_2 \end{bmatrix} - \int_r^1 \begin{bmatrix} Q_{11}(r,s) & Q_{12}(r,s) \\ Q_{21}(r,s) & Q_{22}(r,s) \end{bmatrix}\begin{bmatrix} w_1 \\ w_2 \end{bmatrix}(s,t)\,ds, \tag{57}$$

that transforms the original error system (54)-(56) into the target system

$$\frac{\partial}{\partial t}\begin{bmatrix} w_1 \\ w_2 \end{bmatrix}(r,t) = \frac{\partial^2}{\partial r^2}\begin{bmatrix} w_1 \\ w_2 \end{bmatrix}(r,t) + \begin{bmatrix} \lambda_1 & -\lambda_c \\ \lambda_c & \lambda_2 \end{bmatrix}\begin{bmatrix} w_1 \\ w_2 \end{bmatrix}(r,t), \tag{58}$$

$$\begin{bmatrix} w_1 \\ w_2 \end{bmatrix}(0,t) = 0, \tag{59}$$

$$\frac{\partial}{\partial r}\begin{bmatrix} w_1 \\ w_2 \end{bmatrix}(1,t) = -\frac{1}{2}\begin{bmatrix} w_1 \\ w_2 \end{bmatrix}(1,t). \tag{60}$$

where $\lambda_1, \lambda_2 < 1/4$. For the target system (58) - (60), equilibrium $[w_1^{\mathrm{eq}}, w_2^{\mathrm{eq}}](r) = [0,0]$ is exponentially stable in the L_2-norm and the proof of this statement is as follows. Considering the positive-definite function

$$V(t) = \frac{1}{2}\int_0^1 w_1^2(r,t) + w_2^2(r,t)\mathrm{d}r, \tag{61}$$

taking the time derivate and using integration by parts

$$\begin{aligned}\dot{V}(t) = &-\frac{1}{2}w_1^2(1,t) - \int_0^1 w_{1,r}^2 dr + \lambda_1 \int_0^1 w_1^2 dr \\ &- \frac{1}{2}w_2^2(1,t) - \int_0^1 w_{2,r}^2 dr + \lambda_2 \int_0^1 w_2^2 dr,\end{aligned} \tag{62}$$

using the Poincaré inequality

$$\dot{V}(t) \leq -\left(\frac{1}{4} - \lambda_1\right)\int_0^1 w_1^2 dr - \left(\frac{1}{4} - \lambda_2\right)\int_0^1 w_2^2 dr, \tag{63}$$

$$\leq -\left(\frac{1}{2} - 2\lambda_{\max}\right)V(t), \tag{64}$$

with $\lambda_{\max} = \max(\lambda_1, \lambda_2)$. Comparison principle (Lemma 3.4 in [25]) implies $V(t) \leq V(0)\, e^{-\left(\frac{1}{2}-2\lambda_{\max}\right)t}$ or in terms of the norm $\|w(t)\| = \|w(0)\|\, e^{-\left(\frac{1}{4}-\lambda_{\max}\right)t}$. Then for all $\lambda_1, \lambda_2 < \frac{1}{4}$ equilibrium $[w_1^{\text{eq}}, w_2^{\text{eq}}](r) = [0,0]$ is exponentially stable. Following the procedure in [22] elements of the kernel in (57) are solutions of the PDE

$$Q_{11,rr}(r,s) - Q_{11,ss}(r,s) = \lambda_1 Q_{11}(r,s), \tag{65}$$
$$Q_{12,rr}(r,s) - Q_{12,ss}(r,s) = -\lambda_{\text{c}} Q_{12}(r,s), \tag{66}$$
$$Q_{21,rr}(r,s) - Q_{21,ss}(r,s) = \lambda_{\text{c}} Q_{21}(r,s), \tag{67}$$
$$Q_{22,rr}(r,s) - Q_{22,ss}(r,s) = \lambda_2 Q_{22}(r,s), \tag{68}$$

with boundary conditions

$$Q_{11}(0,s) = 0, \quad Q_{11}(r,r) = \frac{\lambda_1}{2}r, \tag{69}$$
$$Q_{12}(0,s) = 0, \quad Q_{12}(r,r) = -\frac{\lambda_{\text{c}}}{2}r, \tag{70}$$
$$Q_{21}(0,s) = 0, \quad Q_{21}(r,r) = \frac{\lambda_{\text{c}}}{2}r, \tag{71}$$
$$Q_{22}(0,s) = 0, \quad Q_{22}(r,r) = \frac{\lambda_2}{2}r, \tag{72}$$

defined on $D = \{(r,s) | 0 \leq r \leq s \leq 1\}$. Output injection gains are

$$p_{11}^+(r) = -\frac{1}{2}Q_{11}(r,1) - Q_{11,s}(r,1), \tag{73}$$
$$p_{12}^+(r) = -\frac{1}{2}Q_{12}(r,1) - Q_{12,s}(r,1), \tag{74}$$
$$p_{21}^+(r) = -\frac{1}{2}Q_{21}(r,1) - Q_{21,s}(r,1), \tag{75}$$
$$p_{22}^+(r) = -\frac{1}{2}Q_{22}(r,1) - Q_{22,s}(r,1), \tag{76}$$

$$q_{11}^+ = a_{11} + \frac{3-\lambda_1}{2}, \tag{77}$$
$$q_{12}^+ = a_{12} - \frac{\lambda_{\text{c}}}{2}, \tag{78}$$
$$q_{21}^+ = a_{21} + \frac{\lambda_{\text{c}}}{2}, \tag{79}$$
$$q_{22}^+ = a_{22} + \frac{3-\lambda_2}{2}, \tag{80}$$

The Klein-Gordon PDE (65)-(68) has a closed form solution

$$Q_{11}(r,s) = \lambda_1 r \frac{I_1(z_1)}{z_1}, \quad Q_{12}(r,s) = -\lambda_{\text{c}} r \frac{J_1(z_{\text{c}})}{z_{\text{c}}}, \tag{81}$$
$$Q_{21}(r,s) = \lambda_{\text{c}} r \frac{I_1(z_{\text{c}})}{z_{\text{c}}}, \quad Q_{22}(r,s) = \lambda_2 r \frac{I_1(z_2)}{z_2}, \tag{82}$$

where $z_i := z_i(r,s) = \sqrt{\lambda_i(r^2 - s^2)}$, $i \in \{1, \text{c}, 2\}$. Substituting (81)-(82) in (73)-(76)

$$p_{11}(r) = -\frac{\lambda_1 r}{2z_1}\left[I_1(z_1) - \frac{2\lambda_1}{z_1}I_2(z_1)\right], \tag{83}$$
$$p_{12}(r) = +\frac{\lambda_{\text{c}} r}{2z_{\text{c}}}\left[J_1(z_{\text{c}}) - \frac{2\lambda_{\text{c}}}{z_{\text{c}}}J_2(z_{\text{c}})\right], \tag{84}$$
$$p_{21}(r) = -\frac{\lambda_{\text{c}} r}{2z_{\text{c}}}\left[I_1(z_{\text{c}}) - \frac{2\lambda_{\text{c}}}{z_{\text{c}}}I_2(z_{\text{c}})\right], \tag{85}$$
$$p_{22}(r) = -\frac{\lambda_2 r}{2z_2}\left[I_1(z_2) - \frac{2\lambda_2}{z_2}I_2(z_2)\right], \tag{86}$$

where $J_1(\cdot)$, $J_2(\cdot)$, $I_1(\cdot)$ and $I_2(\cdot)$ are first and second order Bessel functions and first and second ortder modified Bessel functions, respectively.

3.4 Inverse Transformation and Un-normalization

An observer in the original coordinates $\widehat{c}_{s,1^+}, \widehat{c}_{s,2^+}$ can be found by inverting transformation (44) and un-normalizing the dimensions (43).

Since the observer for the positive electrode is based on the linear approximation (41) and (42), convergence results hold only locally. However, the linearization and the computation of observer gains can be done continuously (using measurements of surface concentration or their estimates) and the final result is an observer for the nonlinear PDAE of the positive electrode

$$\begin{aligned}\frac{\partial \widehat{c}_{\text{s},1^+}}{\partial t}(r,t) = &\frac{1}{r^2}\frac{\partial}{\partial r}\left[D_{\text{s},1^+} r^2 \frac{\partial \widehat{c}_{\text{s},1^+}}{\partial r}(r,t)\right] \\ &+ \overline{p}_{11}^+(r)\left[c_{\text{ss},1^+}(t) - \widehat{c}_{\text{ss},1^+}(t)\right] \\ &+ \overline{p}_{12}^+(r)\left[c_{\text{ss},2^+}(t) - \widehat{c}_{\text{ss},2^+}(t)\right],\end{aligned} \tag{87}$$

$$\widehat{c}_{\mathrm{s},1^+}(0,t) = 0, \tag{88}$$

$$\begin{aligned} D_{\mathrm{s},1^+}\frac{\partial \widehat{c}_{\mathrm{s},1^+}}{\partial r}(R_{\mathrm{p},1^+},t) &= -\widehat{j}_{\mathrm{n},1^+}(t) \\ &\quad + \overline{q}_{11}^{+}\left[c_{\mathrm{ss},1^+}(t) - \widehat{c}_{\mathrm{ss},1^+}(t)\right] \\ &\quad + \overline{q}_{12}^{+}\left[c_{\mathrm{ss},2^+}(t) - \widehat{c}_{\mathrm{ss},2^+}(t)\right], \end{aligned} \tag{89}$$

$$\begin{aligned} \frac{\partial \widehat{c}_{\mathrm{s},2^+}}{\partial t}(r,t) &= \frac{1}{r^2}\frac{\partial}{\partial r}\left[D_{\mathrm{s},2^+}r^2\frac{\partial \widehat{c}_{\mathrm{s},2^+}}{\partial r}(r,t)\right] \\ &\quad + \overline{p}_{21}^{+}(r)\left[c_{\mathrm{ss},1^+}(t) - \widehat{c}_{\mathrm{ss},1^+}(t)\right] \\ &\quad + \overline{p}_{22}^{+}(r)\left[c_{\mathrm{ss},2^+}(t) - \widehat{c}_{\mathrm{ss},2^+}(t)\right], \end{aligned} \tag{90}$$

$$\widehat{c}_{\mathrm{s},2^+}(0,t) = 0, \tag{91}$$

$$\begin{aligned} D_{\mathrm{s},2^+}\frac{\partial \widehat{c}_{\mathrm{s},2^+}}{\partial r}(R_{\mathrm{p},2^+},t) &= -\widehat{j}_{\mathrm{n},2^+}(t) \\ &\quad + \overline{q}_{21}^{+}\left[c_{\mathrm{ss},1^+}(t) - \widehat{c}_{\mathrm{ss},1^+}(t)\right] \\ &\quad + \overline{q}_{22}^{+}\left[c_{\mathrm{ss},2^+}(t) - \widehat{c}_{\mathrm{ss},2^+}(t)\right], \end{aligned} \tag{92}$$

where $\widehat{j}_{\mathrm{n},1^+}(t)$ and $\widehat{j}_{\mathrm{n},2^+}(t)$ are obtained by solving the nonlinear algebraic equations

$$I(t) = -a_{\mathrm{s},1^+}FL^{+}\widehat{j}_{\mathrm{n},1^+}(t) - a_{\mathrm{s},2^+}FL^{+}\widehat{j}_{\mathrm{n},2^+}(t), \tag{93}$$

$$\begin{aligned} 0 &= -\widehat{\phi}_{\mathrm{s},+}(t) + \widehat{\eta}_{1^+},(t) + U_{1^+}(c_{\mathrm{ss},1^+}(t)) \\ &\quad + R_{\mathrm{f},1^+}F\widehat{j}_{\mathrm{n},1^+}(t), \end{aligned} \tag{94}$$

$$\begin{aligned} 0 &= -\widehat{\phi}_{\mathrm{s},+}(t) + \widehat{\eta}_{2^+},(t) + U_{2^+}(c_{\mathrm{ss},2^+}(t)) \\ &\quad + R_{\mathrm{f},2^+}F\widehat{j}_{\mathrm{n},2^+}(t), \end{aligned} \tag{95}$$

$$\widehat{j}_{\mathrm{n},1^+}(t) = \frac{i_{0,1^+}(t)}{F}\left[e^{\frac{\alpha_{\mathrm{a}}F}{RT}\widehat{\eta}_{1^+}(t)} - e^{-\frac{\alpha_{\mathrm{c}}F}{RT}\widehat{\eta}_{1^+}(t)}\right], \tag{96}$$

$$\widehat{j}_{\mathrm{n},2^+}(t) = \frac{i_{0,2^+}(t)}{F}\left[e^{\frac{\alpha_{\mathrm{a}}F}{RT}\widehat{\eta}_{2^+}(t)} - e^{-\frac{\alpha_{\mathrm{c}}F}{RT}\widehat{\eta}_{2^+}(t)}\right]. \tag{97}$$

Observer gains are

$$\overline{p}_{11}^{+}(r) = -\frac{\lambda_1 D_{\mathrm{s},1^+}}{2R_{\mathrm{p},1^+}^2\overline{z}_1}\left[I_1(\overline{z}_1) - \frac{2\lambda_1}{\overline{z}_1}I_2(\overline{z}_1)\right], \tag{98}$$

$$\overline{p}_{12}^{+}(r) = +\frac{\lambda_{\mathrm{c}} D_{\mathrm{s},1^+}}{2R_{\mathrm{p},1^+}^2\overline{z}_{\mathrm{c}}}\left[J_1(\overline{z}_{\mathrm{c}}) - \frac{2\lambda_c}{\overline{z}_{\mathrm{c}}}J_2(\overline{z}_{\mathrm{c}})\right], \tag{99}$$

$$\overline{p}_{21}^{+}(r) = -\frac{\lambda_{\mathrm{c}} D_{\mathrm{s},2^+}}{2R_{\mathrm{p},2^+}^2\overline{z}_{\mathrm{c}}}\left[I_1(\overline{z}_{\mathrm{c}}) - \frac{2\lambda_c}{\overline{z}_c}I_2(\overline{z}_c)\right], \tag{100}$$

$$\overline{p}_{22}^{+}(r) = -\frac{\lambda_2 D_{\mathrm{s},2^+}}{2R_{\mathrm{p},2^+}^2\overline{z}_2}\left[I_1(\overline{z}_2) - \frac{2\lambda_2}{\overline{z}_2}I_2(\overline{z}_2)\right], \tag{101}$$

with $\overline{z}_j := \overline{z}_j(r) = \sqrt{\lambda_j\left(\frac{r^2}{R_{\mathrm{p},i^+}^2} - 1\right)}$ and

$$\overline{q}_{11}^{+} = \rho_{11} + \frac{D_{\mathrm{s},1^+}(3-\lambda_1)}{2R_{\mathrm{p},1^+}}, \tag{102}$$

$$\overline{q}_{12}^{+} = \rho_{12} - \frac{D_{\mathrm{s},1^+}\lambda_{\mathrm{c}}}{2R_{\mathrm{p},1^+}}, \tag{103}$$

$$\overline{q}_{21}^{+} = \rho_{21} + \frac{D_{\mathrm{s},2^+}\lambda_{\mathrm{c}}}{2R_{\mathrm{p},2^+}}, \tag{104}$$

$$\overline{q}_{22}^{+} = \rho_{22} + \frac{D_{\mathrm{s},2^+}(3-\lambda_2)}{2R_{\mathrm{p},2^+}}. \tag{105}$$

3.5 Observer for Negative Electrode

The observer for the negative electrode consists of a copy of the plant and surface concentration error injection from the positive electrode as follows

$$\begin{aligned} \frac{\partial \widehat{c}_{\mathrm{s},1^-}}{\partial t}(r,t) &= \frac{1}{r^2}\frac{\partial}{\partial r}\left[D_{\mathrm{s},1^-}r^2\frac{\partial \widehat{c}_{\mathrm{s},1^-}}{\partial r}(r,t)\right] \\ &\quad + \overline{p}_{1}^{-}(r)\left[c_{\mathrm{ss},1^+}(t) - \widehat{c}_{\mathrm{ss},1^+}(t)\right] \\ &\quad + \overline{p}_{2}^{-}(r)\left[c_{\mathrm{ss},2^+}(t) - \widehat{c}_{\mathrm{ss},2^+}(t)\right], \end{aligned} \tag{106}$$

$$\widehat{c}_{\mathrm{s},1^-}(0,t) = 0, \tag{107}$$

$$\begin{aligned} D_{\mathrm{s},1^-}\frac{\partial \widehat{c}_{\mathrm{s},1^-}}{\partial r}(R_{\mathrm{p},1^-},t) &= -\frac{I(t)}{Fa^{-}L} + \overline{q}_{1}^{-}\left[c_{\mathrm{ss},1^+}(t) - \widehat{c}_{\mathrm{ss},1^+}(t)\right] \\ &\quad + \overline{q}_{2}^{-}\left[c_{\mathrm{ss},2^+}(t) - \widehat{c}_{\mathrm{ss},2^+}(t)\right]. \end{aligned} \tag{108}$$

Observer gains $\overline{p}_1^{-}(r), \overline{p}_2^{-}(r), \overline{q}_1^{-}$ and $\overline{q}_2^{-}$ are selected such that $\frac{d}{dt}\widehat{n}_{\mathrm{Li,s}}(t) = 0$. This property holds true under the following relations between the estimation gains

$$0 = a_{\mathrm{s},1^+}L^{+}D_{\mathrm{s},1^+}\overline{q}_{11}^{+} + a_{\mathrm{s},2^+}L^{+}D_{\mathrm{s},2^+}\overline{q}_{21}^{+} + a_{\mathrm{s},1^-}L^{-}D_{\mathrm{s},1^-}\overline{q}_{1}^{-}, \tag{109}$$

$$0 = a_{\mathrm{s},1^+}L^{+}D_{\mathrm{s},1^+}\overline{q}_{12}^{+} + a_{\mathrm{s},2^+}L^{+}D_{\mathrm{s},2^+}\overline{q}_{22}^{+} + a_{\mathrm{s},1^-}L^{-}D_{\mathrm{s},1^-}\overline{q}_{2}^{-}, \tag{110}$$

$$\begin{aligned} 0 &= \frac{a_{\mathrm{s},1^+}L^{+}}{R_{\mathrm{p},1^+}^2}\int_0^{R_{\mathrm{p},1^+}} r^2\overline{p}_{11}^{+}(r)dr + \frac{a_{\mathrm{s},2^+}L^{+}}{R_{\mathrm{p},2^+}^2}\int_0^{R_{\mathrm{p},2^+}} r^2\overline{p}_{21}^{+}(r)dr \\ &\quad + \frac{a_{\mathrm{s},1^-}L^{-}}{R_{\mathrm{p},1^-}^2}\int_0^{R_{\mathrm{p},1^-}} r^2\overline{p}_{1}^{-}(r)dr, \end{aligned} \tag{111}$$

$$\begin{aligned} 0 &= \frac{a_{\mathrm{s},1^+}L^{+}}{R_{\mathrm{p},1^+}^2}\int_0^{R_{\mathrm{p},1^+}} r^2\overline{p}_{12}^{+}(r)dr + \frac{a_{\mathrm{s},2^+}L^{+}}{R_{\mathrm{p},2^+}^2}\int_0^{R_{\mathrm{p},2^+}} r^2\overline{p}_{22}^{+}(r)dr \\ &\quad + \frac{a_{\mathrm{s},1^-}L^{-}}{R_{\mathrm{p},1^-}^2}\int_0^{R_{\mathrm{p},1^-}} r^2\overline{p}_{2}^{-}(r)dr, \end{aligned} \tag{112}$$

There are multiple solutions for gains $\overline{p}_1^-(r)$ and $\overline{p}_2^-(r)$ but constant gains can be found easily

$$\overline{p}_1^- = -\frac{\frac{a_{s,1^+}L^+}{R_{p,1^+}^2}\int_0^{R_{p,1^+}} r^2\overline{p}_{11}^+(r)dr + \frac{a_{s,2^+}L^+}{R_{p,2^+}^2}\int_0^{R_{p,2^+}} r^2\overline{p}_{21}^+(r)dr}{\varepsilon_{s,1^-}L^-}, \tag{113}$$

$$\overline{p}_2^- = -\frac{\frac{a_{s,1^+}L^+}{R_{p,1^+}^2}\int_0^{R_{p,1^+}} r^2\overline{p}_{12}^+(r)dr + \frac{a_{s,2^+}L^+}{R_{p,2^+}^2}\int_0^{R_{p,2^+}} r^2\overline{p}_{22}^+(r)dr}{\varepsilon_{s,1^-}L^-}, \tag{114}$$

and

$$\overline{q}_1^- = -\frac{a_{s,1^+}L^+D_{s,1^+}\overline{q}_{11}^+ + a_{s,2^+}L^+D_{s,2^+}\overline{q}_{21}^+}{a_{s,1^-}L^-D_{s,1^-}}, \tag{115}$$

$$\overline{q}_2^- = -\frac{a_{s,1^+}L^+D_{s,1^+}\overline{q}_{12}^+ + a_{s,2^+}L^+D_{s,2^+}\overline{q}_{22}^+}{a_{s,1^-}L^-D_{s,1^-}}. \tag{116}$$

The observer is initialized with the correct value of lithium in the solid phase, $n_{\mathrm{Li,s}}$ in (32), assuming it is known beforehand, i.e.

$$n_{\mathrm{Li,s}} = \sum_i \frac{\varepsilon_{s,i}L_i}{\frac{4}{3}\pi R_{p,i}^3}\int_0^{R_{p,i}} 4\pi r^2\hat{c}_{s,i}(r,0)dr. \tag{117}$$

4 Simulation

For the simulation presented in this section, one particle in the negative electrode and two particles in the positive electrode are being considered. Simulation results are shown in Fig. 3 with $\lambda_1 = \lambda_2 = -10$ and $\lambda_c = 10^{-8}$. From top to bottom, the first plot shows the current density profile used in this test which is obtained from the urban dynamometer driving schedule (UDDS) and is representative of the battery use in automotive applications. The second plot shows the estimation error in the output voltage and since measurements are being generated from a SPM, convergence is expected. The third plot shows the real and estimated (normalized) surface concentrations in the two particles of the positive electrode. Finally, the fourth plot shows the real and estimated (normalized) surface concentration in the particle of negative electrode. Here, perfect knowledge of surface concentration in particles of the positive electrode is assumed. For battery management applications values of surface concentration in the positive electrode could be estimated from current and voltage measurements [15, 20, 23]. Initial estimates of lithium concentration are chosen with the correct value of n_{Li} (i.e. condition in (117) is satisfied).

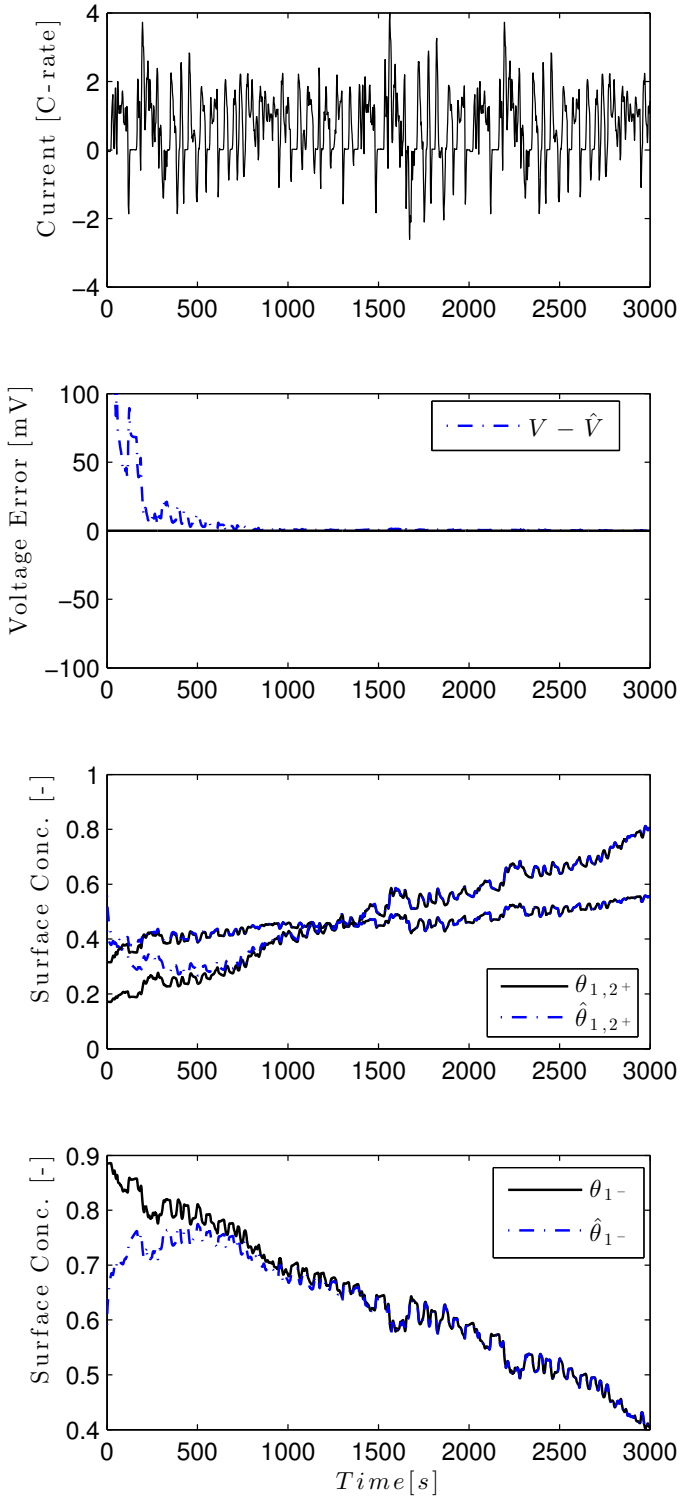

FIGURE 3. SIMULATION. Perfect measurement of surface concentration is used from a single particle model and current density (input) is obtained fromUDDS. Initial estimates of lithium concentration are chosen with the correct value of n_{Li} (i.e. condition in (117) is satisfied). Normalized values of real and estimated surface concentration are plotted i.e. $\theta_i = c_{ss,i}(t)/c_{\max,s,i}$

5 Conclusions

An observer for a system of diffusion equations appearing in a single particle model of lithium-ion batteries with electrodes of multiple active materials has been derived in this paper. The observer is based on the backstepping method for PDEs and is an extension of previous backtepping observers designed only for single active materials. Simulations where presented showing the effectiveness of the estimation scheme. This observer could be used for other settings apart from the multiple material problem, for example in electrodes with a unique active material (i.e. same OCP functions and all parameters with same values) but with two or more distinct particle sizes (i.e. different R_{p}). An important limitation of the observer is that, since it is derived from a reduced electrochemical model, convergence is only expected in the cases when this reduced model is an appropriate approximation of the full electrochemical model (or battery). Future work includes the test of this observer against the full electrochemical model and the extension to simultaneous parameter and state estimation.

The authors would like to acknowledge the support from ARPA-E (AMPED).

6 Nomenclature

TABLE 1. **States and Variables**

c_{s}	Concentration of lithium ions in particles
c_{ss}	Surface concentration in particles
θ	Normalized surface concentration
j_n	Molar ion flux
i_0	Exchange current density
η	Overpotential
c_{e}	Concentration of lithium ions in electrolyte
ϕ_{s}	Electric potential in the solid electrodes
ϕ_{e}	Electric potential in the electrolyte
i_{e}	Ionic current density
$f_{\mathrm{c/a}}$	Activity coefficient in the electrolyte
U	Open circuit potential functions
I	Current density (input)
V	Voltage (output)

TABLE 2. **Parameters and Constants**

D_{s}	Diffusion coefficient in solid particles
R_{p}	Particle radius
n^-, n^+	Number of active materials in electrodes
α_a, α_c	Transport coefficients
R	Gas constant
T	Constant temperature
F	Faraday constant
k	Effective reaction rate
$c_{\mathrm{s}}^{\max}$	Maximum concentration
R_{f}	Film resistance
ε_{s}	Volume fraction of active material
ε_{e}	Volume fraction of electrolyte
a_{s}	Specific interfacial area
D_{e}	Diffusion coefficient in electrolyte
σ	Conductivity in solid electrodes
κ	Conductivity in electrolyte
t_{c}^0	Transference number
L	Length of region
$c_{\mathrm{e},0}$	Constant approximation of c_{e}
n_{Li}	Total lithium in solid particles (per unit area)

REFERENCES

[1] Chaturvedi, N., Klein, R., Christensen, J., Ahmed, J., and Kojic, A., 2010. "Algorithms for Advanced Battery-Management Systems". *IEEE Control Systems Magazine,* ***30***(3), June, pp. 49–68.

[2] Siegel, J. B., Lin, X., Stefanopoulou, A. G., Hussey, D. S., Jacobson, D. L., and Gorsich, D., 2011. "Neutron imaging of lithium concentration in lfp pouch cell battery". *Journal of the Electrochemical Society,* ***158***(5), pp. A523–A529.

[3] Thomas, K. E., Newman, J., and Darling, R. M., 2002. "Mathematical Modeling of Lithium Batteries". In *Advances in Lithium-Ion Batteries*, W. A. van Schalkwijk and B. Scrosati, eds. Springer US, Boston, MA, pp. 345–392.

[4] Albertus, P., Christensen, J., and Newman, J., 2009. "Experiments on and Modeling of Positive Electrodes with Multiple Active Materials for Lithium-Ion Batteries". *Journal of The Electrochemical Society,* ***156***(7), p. A606.

[5] Myung, S.-T., Cho, M. H., Hong, H. T., Kang, T. H., and

Kim, C.-S., 2005. "Electrochemical evaluation of mixed oxide electrode for li-ion secondary batteries: Li 1.1 mn 1.9 o 4 and lini 0.8 co 0.15 al 0.05 o 2". *Journal of power sources,* ***146***(1), pp. 222–225.

[6] Hu, X., Li, S., and Peng, H., 2012. "A comparative study of equivalent circuit models for Li-ion batteries". *Journal of Power Sources,* ***198***, Jan., pp. 359–367.

[7] Plett, G. L., 2004. "Extended Kalman filtering for battery management systems of LiPB-based HEV battery packs". *Journal of Power Sources,* ***134***(2), Aug., pp. 277–292.

[8] Yiran Hu, and Yurkovich, S., 2010. "Battery state of charge estimation in automotive applications using LPV techniques". IEEE, pp. 5043–5049.

[9] IL-Song Kim, 2010. "A Technique for Estimating the State of Health of Lithium Batteries Through a Dual-Sliding-Mode Observer". *IEEE Transactions on Power Electronics,* ***25***(4), Apr., pp. 1013–1022.

[10] Bashash, S., and Fathy, H. K., 2013. "Battery State of Health and Charge Estimation Using Polynomial Chaos Theory". ASME, p. V001T05A006.

[11] Plett, G. L., 2006. "Sigma-point Kalman filtering for battery management systems of LiPB-based HEV battery packs". *Journal of Power Sources,* ***161***(2), Oct., pp. 1369–1384.

[12] Saha, B., Goebel, K., Poll, S., and Christophersen, J., 2009. "Prognostics Methods for Battery Health Monitoring Using a Bayesian Framework". *IEEE Transactions on Instrumentation and Measurement,* ***58***(2), Feb., pp. 291–296.

[13] Santhanagopalan, S., and White, R. E., 2006. "Online estimation of the state of charge of a lithium ion cell". *Journal of Power Sources,* ***161***(2), Oct., pp. 1346–1355.

[14] Di Domenico, D., Fiengo, G., and Stefanopoulou, A., 2008. "Lithium-ion battery state of charge estimation with a Kalman Filter based on a electrochemical model". IEEE, pp. 702–707.

[15] Moura, S. J., Chaturvedi, N. A., and Krstic, M., 2013. "Adaptive Partial Differential Equation Observer for Battery State-of-Charge/State-of-Health Estimation Via an Electrochemical Model". *Journal of Dynamic Systems, Measurement, and Control,* ***136***(1), Oct., p. 011015.

[16] Dey, S., and Ayalew, B., 2014. "Nonlinear observer designs for state-of-charge estimation of Lithium-ion batteries". IEEE, pp. 248–253.

[17] Khaleghi Rahimian, S., Rayman, S., and White, R. E., 2013. "Extension of physics-based single particle model for higher charge-discharge rates". *Journal of Power Sources,* ***224***, Feb., pp. 180–194.

[18] Kemper, P., and Kum, D., 2013. "Extended Single Particle Model of Li-Ion Batteries Towards High Current Applications". IEEE, pp. 1–6.

[19] Tanim, T. R., Rahn, C. D., and Wang, C.-Y., 2015. "State of charge estimation of a lithium ion cell based on a temperature dependent and electrolyte enhanced single particle model". *Energy,* ***80***, Feb., pp. 731–739.

[20] Moura, S. J., Bribiesca Argomedo, F., Reinhardt, K., Mirtabatabaei, A., and Miroslav, K., 2016. "Battery State Estimation for a Single Particle Model with Electrolyte Dynamics". *escholarship*.

[21] Bartlett, A., Marcicki, J., Onori, S., Rizzoni, G., Yang, X. G., and Miller, T., 2014. "Electrochemical model-based state of charge and capacity estimation for a composite electrode lithium-ion battery".

[22] Krstic, M., Smyshlyaev, A., and Society for Industrial and Applied Mathematics, 2008. *Boundary control of PDEs a course on backstepping designs*. Society for Industrial and Applied Mathematics, Philadelphia, Pa.

[23] Moura, S. J., Chaturvedi, N. A., and Krstic, M., 2012. "PDE estimation techniques for advanced battery management systems—Part I: SOC estimation". IEEE, pp. 559–565.

[24] Klein, R., Chaturvedi, N. A., Christensen, J., Ahmed, J., Findeisen, R., and Kojic, A., 2013. "Electrochemical Model Based Observer Design for a Lithium-Ion Battery". *IEEE Transactions on Control Systems Technology,* ***21***(2), Mar., pp. 289–301.

[25] Khalil, H. K., 2002. *Nonlinear systems*, 3rd ed. Prentice Hall, Upper Saddle River, N.J.